Published paper

Flinn, L.J, Keatinge, M, Bretaud, S, Mortiboys, H, Matsui, H, De Felice, E, Woodroof, H.I, Brown, L, McTighe, A, Soellner, R, Allen, C.E, Heath, P.R, Milo, M, Muqit, M.M.K, Reichert, A.S, Koester, R.W, Ingham, P.W and Bandmann, O (2013) TigarB Causes Mitochondrial Dysfunction and Neuronal Loss in PINK1 Deficiency. Annals of Neurology, 74 (6). 837 – 847. Doi: 10.1002/ana.23999

TigarB Causes Mitochondrial Dysfunction and Neuronal Loss in PINK1 Deficiency

Laura J. Flinn, PhD,[1,2] Marcus Keatinge, MBiolSci,[1,2] Sandrine Bretaud, PhD,[1,2] Heather Mortiboys, PhD,[2] Hideaki Matsui, PhD,[3] Elena De Felice, PhD,[1,2,4] Helen I. Woodroof, BSc Hons,[5] Lucy Brown, MBChB,[1,2] Aimee McTighe, MBiolSci,[1,2] Rosemarie Soellner, PhD,[6] Claire E. Allen, PhD,[1] Paul R. Heath, PhD,[2] Marta Milo, PhD,[6] Miratul M. K. Muqit, PhD,[5,7] Andreas S. Reichert, PhD,[8,9] Reinhard W. Köster, PhD,[3,6] Philip W. Ingham, PhD,[1,10] and Oliver Bandmann, MD, PhD[1,2]

Objective: Loss of function mutations in PINK1 typically lead to early onset Parkinson disease (PD). Zebrafish (*Danio rerio*) are emerging as a powerful new vertebrate model to study neurodegenerative diseases. We used a *pink1* mutant ($pink^{-/-}$) zebrafish line with a premature stop mutation (Y431*) in the PINK1 kinase domain to identify molecular mechanisms leading to mitochondrial dysfunction and loss of dopaminergic neurons in PINK1 deficiency.
Methods: The effect of PINK1 deficiency on the number of dopaminergic neurons, mitochondrial function, and morphology was assessed in both zebrafish embryos and adults. Genome-wide gene expression studies were undertaken to identify novel pathogenic mechanisms. Functional experiments were carried out to further investigate the effect of PINK1 deficiency on early neurodevelopmental mechanisms and microglial activation.
Results: PINK1 deficiency results in loss of dopaminergic neurons as well as early impairment of mitochondrial function and morphology in *Danio rerio*. Expression of *TigarB*, the zebrafish orthologue of the human, TP53-induced glycolysis and apoptosis regulator *TIGAR*, was markedly increased in $pink^{-/-}$ larvae. Antisense-mediated inactivation of *TigarB* gave rise to complete normalization of mitochondrial function, with resulting rescue of dopaminergic neurons in $pink^{-/-}$ larvae. There was also marked microglial activation in $pink^{-/-}$ larvae, but depletion of microglia failed to rescue the dopaminergic neuron loss, arguing against microglial activation being a key factor in the pathogenesis.
Interpretation: $Pink1^{-/-}$ zebrafish are the first vertebrate model of PINK1 deficiency with loss of dopaminergic neurons. Our study also identifies TIGAR as a promising novel target for disease-modifying therapy in PINK1-related PD.
ANN NEUROL 2013;74:837–847

Autosomal recessively inherited, loss of function mutations in PTEN-induced kinase 1 (*PINK1*) typically lead to early onset Parkinson disease (EOPD).[1] The PINK1 protein is expressed ubiquitously throughout the human brain.[2] Impaired mitochondrial function and morphology have been described in both human *PINK1* mutant patient tissue and different PINK1-deficient in vitro or in vivo model systems.[3,4] PINK1 has also been implicated in oxidative stress defense, mitophagy, and the regulation of mitochondrial calcium homeostasis.[3–5]

View this article online at wileyonlinelibrary.com. DOI: 10.1002/ana.23999

Received Nov 29, 2012, and in revised form Jul 30, 2013. Accepted for publication Aug 3, 2013.

Address correspondence to Dr Bandmann, Sheffield Institute for Translational Neuroscience, Department of Neuroscience, University of Sheffield, 385a Glossop Road, Sheffield S10 2HQ, United Kingdom. E-mail: o.bandmann@sheffield.ac.uk

From the [1]Medical Research Council Centre for Developmental and Biomedical Genetics, University of Sheffield, Sheffield, United Kingdom; [2]Sheffield Institute for Translational Neuroscience, Department of Neuroscience, University of Sheffield, Sheffield, United Kingdom; [3]Zoological Institute, Braunschweig University of Technology, Braunschweig, Germany; [4]Department of Morphology, Biochemistry, Physiology, and Animal Productions, Section of Morphology, University of Messina, Polo Universitario dell'Annunziata, Messina, Italy; [5]Medical Research Council Protein Phosphorylation and Ubiquitylation Unit, College of Life Sciences, University of Dundee, Dundee, United Kingdom; [6]Helmholtz Center, Institute of Developmental Genetics, Munich, Germany; [7]College of Medicine, Dentistry, and Nursing, University of Dundee, Dundee, United Kingdom; [8]Department of Mitochondrial Biology, Buchmann Institute for Molecular Life Sciences, Frankfurt am Main, Germany; [9]Department of Mitochondrial Biology, Center for Molecular Medicine, Goethe University, Frankfurt am Main, Germany; [10]Lee Kong Chian School of Medicine, Nanyang Technological University/Imperial College London, Singapore.

Additional supporting information can be found in the online version of this article.

However, the precise mechanisms leading to neuronal cell death remain unclear. *Pink1* knockout mice do not develop loss of dopamine (DA) neurons in the substantia nigra and can therefore only be of limited use in investigating the mechanisms leading to neuronal cell death in human Parkinson disease (PD).[6]

Zebrafish are increasingly being used to model neurodegenerative diseases.[7] As vertebrates, they are closer to humans than other genetically tractable model organisms such as *Drosophila* or *Caenorhabditis elegans*. Zebrafish embryos develop externally, are transparent, and have a well-characterized DA nervous system.[8] To date, investigations of the functional consequences of PD gene dysfunction in zebrafish have relied on the injection of morpholino antisense oligonucleotides (MOs).[7] A major limitation of this approach is that MOs injected into the fertilized egg lose their effect within 3 to 5 days postfertilization, thus precluding investigation of the morphological, biochemical, or behavioral effects of gene dysfunction at larval and adult stages. In addition, morpholinos are frequently associated with nonspecific, off-target effects.[9] Previous studies using the MO strategy to investigate the effects of PINK1 deficiency in zebrafish have led to conflicting results.[10–12]

Using the targeting induced local lesions in genomes (TILLING) approach, we have now established a stable line carrying a premature stop mutation in the kinase-encoding domain of *pink1* (Y431*), the zebrafish orthologue of human *PINK1*. We provide confirmation that this mutation leads to inactivation of PINK1 catalytic activity and decreased mRNA stability. We further demonstrate that PINK1 deficiency in *Danio rerio* results in highly specific abnormalities in early development, which closely match the biochemical and morphological manifestations of the human disease, with persisting loss of dopaminergic neurons in adulthood and also persisting mitochondrial impairment. Genome-wide gene expression studies identified upregulation of *TigarB*, the zebrafish homologue of the TP53-induced glycolysis and apoptosis regulator (TIGAR).[13] Remarkably, *TigarB* knockdown resulted in normalization of mitochondrial function and complete rescue of ascending dopaminergic neurons. Modulation of TIGAR-related mechanisms may therefore be a promising novel strategy to develop disease-modifying therapy for PINK1-related PD.

Materials and Methods

All zebrafish husbandry and experimental procedures were performed in accordance with the UK Home Office Animals (Scientific Procedures) Act (project license PPL 40/3402). Details of animal maintenance, mutagenesis, and identification of the described *pink1* mutation are summarized in the Supplementary Materials and Methods.

In Vitro Kinase Assay of PINK1 and mRNA Stability

All PINK1 enzymes used in this study were expressed in *Escherichia coli* as full-length maltose-binding protein fusion proteins as previously described.[14] Briefly, BL21 codon$^+$ transformants were grown at 37°C then shifted to 16°C and induced with 250μM isopropyl β-D-thiogalactoside at OD_{600} = 0.5. Cultures were then grown for a further 15 to 16 hours at 16°C. Cells were lysed by sonication, and lysates were clarified by centrifugation at 30,000 $\times$ *g* for 30 minutes at 4°C followed by incubation with 1ml per liter of culture of amylose resin for 1.5 hours at 4°C. The resin was washed thoroughly, and proteins were then eluted and dialyzed overnight at 4°C into storage buffer. Kinase assays were set up in a volume of 40μl, with substrates at 2μM and all kinases at 1μg in 50mM Tris-HCl (pH 7.5), 0.1mM ethyleneglycoltetraacetic acid, 10mM $MgCl_2$, 2mM dithiothreitol, and 0.1mM [γ-^{32}P]adenosine triphosphate (ATP). Assays were incubated at 30°C with shaking at 1,200rpm and terminated after 30 minutes by addition of sodium dodecyl sulfate (SDS) sample buffer. Reaction mixtures were resolved by SDS–polyacrylamide gel electrophoresis. Proteins were detected by Coomassie staining, and incorporation of [γ-^{32}P]ATP into substrates was analyzed by autoradiography.

RNA was extracted from *wt* and *pink1*$^{-/-}$ embryos at 3 days postfertilization (dpf). A Verso cDNA synthesis kit (Thermo Scientific, Waltham, MA) was used to generate the cDNA. Transcript levels of *pink1* were quantified by quantitative polymerase chain reaction (qPCR) using primers R (5′-CTGATGACGTTCAGCTGGTG) and L (5′-CCACAGACTGATGTGCAGGA) at an annealing temperature of 60°C.

Quantification of Dopaminergic Neurons in Zebrafish Larvae and Adult Brains

Whole mount tyrosine hydroxylase (TH) and DA transport protein (DAT) in situ hybridization was undertaken as previously described.[15] The mean number of these diencephalic dopaminergic neurons for *wt* and *pink1*$^{-/-}$ was calculated over 3 independent experiments (n = 10 of embryos per genotype and experiment). Nine adult *pink1*$^{-/-}$ and a further 9 wild-type controls (wild-type siblings) were sacrificed at the age of 18 months. The number of dopaminergic neurons in these adult brains was determined by counting the number of TH-positive neurons in axial sections within the DC3 and DC4 cluster (see Supplementary Materials and Methods for further details).

Mitochondrial Respiratory Chain Assays and Analysis of Mitochondrial Morphology

Mitochondrial respiratory chain assays were undertaken as previously described.[16] Larvae were harvested at 5 dpf (~30 per sample) for initial assessment of mitochondrial function and at 3 dpf to determine the effect of *TigarB* knockdown on mitochondrial function (see below). Mitochondrial respiratory

complexes were measured in adult muscle tissue of 24-month-old *pink1*$^{-/-}$ and *wt* zebrafish. Mitochondrial morphology was assessed at 5 dpf in larvae and at 18 months in adult muscle tissue (see Supplementary Materials and Methods for further details).

Neurodevelopmental Markers

In situ hybridization was undertaken using probes for *Emx1,* sonic hedgehog *(shh), Pax2.1, Krox20,* and *Otpa/Otpb*. Embryos were fixed at 24 hours postfertilization (hpf), mounted in glycerol, and photographed using a Zeiss Axioplan microscope (Carl Zeiss, Oberkochen, Germany). All experiments were done in triplicate; a minimum of 10 embryos were used for each genotype per experiment. Islet-1 antibody staining was carried out at 24 hpf as described previously.[16]

mRNA Microarray Expression Analysis

RNA was extracted from *pink1*$^{-/-}$ and *wt* at 5 dpf. RNA samples were labeled and hybridized to Agilent *Danio rerio* 4 × 44K arrays following the manufacturer's protocols (Agilent Technologies, Santa Clara, CA). These data were then analyzed using GeneSpring GX (Agilent), and significant differentially expressed probes were defined as those with a probability value < 0.01 (determined by a *t* test against zero, using the Benjamini–Hochberg correction for multiple comparisons) as well as fold-change between *wt* and mutant > 2.0 (see Supplementary Materials and Methods for further details).

qPCR, In Situ Hybridization, and Knockdown of TigarB

A detailed description of the *TigarB* qPCR and in situ hybridization and MO-mediated *TigarB* knockdown is provided in the Supplementary Materials and Methods. The sequence of the *TigarB* MO (TBMO2) was 5′-TAGAGTGTTTATCTACC TTGCAGCA. The efficacy of the MO was determined by reverse transcriptase PCR (RT-PCR; forward: 5′-GACCAGTA TTATGCTCACATTTGC-3′ and reverse 5′-TCTACAGGCTT GACCTGCTG-3′) and gel electrophoresis (see Supplementary Fig 1). For confirmatory experiments, a *pink1* MO was designed to the exon–intron boundary of exon 5, referred to as PINK5 (PINK5 sequence: 5′-AGAGTCTCTGAGCTCTTAC TGTTGT). Efficacy was determined using primers forward 5′-CTGACTTTGAACGGGCACTT and reverse 5′-TCAGGT GCCATTAGACAGGA. RT-PCR was always performed at 3 dpf on cDNA from control MO-injected, PINK5-injected, and coinjected PINK5 + TBMO2 to confirm the knockdown effect of PINK5. For the coinjection, 7.5ng PINK5 and 7.5ng TBMO2 were injected simultaneously at single cell stage. RT-PCR was performed during every technical replicate to determine the efficacy for both MOs (see also Supplementary Fig 2).

Detection and Inactivation of Microglia

Microglial cells were stained using an in situ probe for apolipoprotein E (ApoE) as previously described.[17] The microglial cells were then counted in *pink*$^{-/-}$ zebrafish larvae and *wt* controls at 72 hpf, using a Zeiss Axioplan microscope.

An MO against the myeloid transcription factor *pu.1* was injected at single cell stage to inhibit macrophage maturation and thus inactivate microglial cells as previously described.[18] The number of activated microglial cells was then counted in anti-*pu.1* MO-injected and uninjected *pink1*$^{-/-}$ larvae as described above.

Statistical Analysis

All experiments were undertaken in triplicate unless specifically stated otherwise. Data represent the mean ± standard error of the mean. A minimum of 10 embryos were used per genotype for each replicate experiment. Each treatment group was normalized to the appropriate wild-type control group, and results were expressed as a percentage of control group mean. One-way analysis of variance and *t* tests of significance were used unless stated otherwise as measures of significance (Prism, version 5.0; GraphPad Software, La Jolla, CA).

Results

TILLING Identifies a Truncating Mutation in pink1 (Y431*)

An *N*-ethyl-*N*-nitrosourea (ENU) mutagenized library was screened for mutations in exons 3, 4, 5, 6, and 7, encoding the kinase domain of the zebrafish *pink1* homologue. A heterozygous male was identified from the SM0604 library with a T to G change at position 1,405 in NM_001008628 (chr23:37574658) in exon 7 (Fig 1A), resulting in a change from tyrosine to a stop codon at position 431 (Y431*) toward the end of the kinase domain (see Fig 1B). The mutation was confirmed with a second, independent method (*DdeI* restriction digest, data not shown). All experiments and results reported in this publication were performed on Y431* mutant fish from the F4 or subsequent generations.

Y431X Mutation Leads to Loss of PINK1 Catalytic Activity and Decreased mRNA Stability

We next investigated the effect of the identified Y431X truncating mutation on PINK1 kinase activity. We initially analyzed this mutation in zebrafish PINK1; however, we were unable to detect any kinase activity of full-length wild-type zebrafish PINK1 in vitro (Supplementary Fig 3). It has previously been demonstrated that an insect orthologue, *Tribolium castaneum* PINK1 (TcPINK1), exhibits robust kinase activity in vitro as judged by phosphorylation of substrates including myelin basic protein (MBP) and the ubiquitinlike (Ubl) domain of parkin at serine 65.[14,19] We therefore modeled the zebrafish Y431X into TcPINK1 (equivalent to Y419X) and determined the effect on kinase activity. We found that the Y419X mutation abolished TcPINK1 activity against the parkin Ubl domain (see Fig 1C) and MBP (Supplementary Fig 4). This is consistent with a previous study that showed that the C terminus of PINK1 is essential for kinase activity.[14] We also hypothesized that

the Y431X mutation results in decreased mRNA stability due to nonsense-mediated decay. As predicted, comparison of *pink1* transcript levels in *wt* and *pink1*$^{-/-}$ embryos revealed a marked decrease of the *pink1*$^{-/-}$ transcript by approximately 65% ($p < 0.0001$) compared to *pink1* transcript levels in *wt* embryos (see Fig 1D).

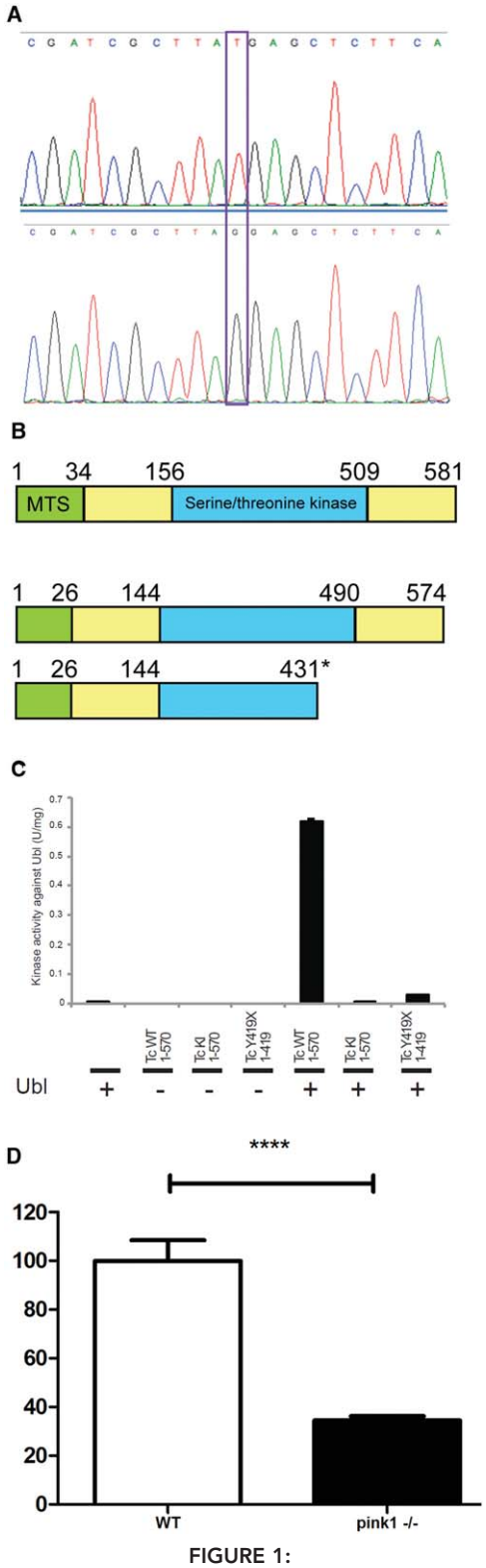

FIGURE 1:

Pink1$^{-/-}$ *Mutants Have Persistent Loss of Dopaminergic Neurons*

Using in situ hybridization with an antisense RNA probe for TH, we analyzed the effect of loss of *pink1* on diencephalic dopaminergic neurons at 5 dpf. The analysis concentrated on particular subgroups of dopaminergic neurons within the diencephalon, namely populations 1, 2, 4, and 5 in the Rink–Wullimann terminology, which are thought to contain ascending dopaminergic neurons analogous to those in the mammalian substantia nigra.[20,21] The number of such ascending diencephalic dopaminergic neurons was reduced by approximately 25% in *pink1*$^{-/-}$ larvae ($p < 0.05$; Fig 2). To confirm that the loss of TH positivity was due specifically to cell loss and not only a reduction of TH gene expression, we also performed in situ hybridization using another marker of dopaminergic neurons, namely DAT. At 5 dpf, the number of DAT^{+} diencephalic neurons in *pink1*$^{-/-}$ larvae was reduced by approximately 30% when compared to *wt* ($p < 0.01$; see Fig 2D), providing supporting evidence for loss of diencephalic dopaminergic neurons in *pink1*$^{-/-}$ larvae. We next determined whether this reduction in dopaminergic neurons persists to adulthood. Two different clusters of dopaminergic neurons were analyzed, namely the DC3 and DC4 clusters. TH^{+} neurons in the DC3 cluster are located in the hypothalamus and project locally; TH^{+} neurons in the DC4 cluster are located in the posterior tuberculum and have long axonal projections to different regions in the brain and spinal cord, including the telencephalon.[22] There was a marked reduction in the number of ascending dopaminergic neurons in the DC4 cluster (*wt* 21.9 ± 5.9 cells, *pink1*$^{-/-}$ 12.0 ± 6.3 cells, $p < 0.01$; Fig 3); the reduction in the DC3 cluster failed to reach statistical significance (*wt* 28.2 ± 4.5 cells, *pink1*$^{-/-}$ 17.7 ± 4.5 cells, $p > 0.05$). The

FIGURE 1: Gene and mutation profile of PINK1^{Y431*} zebrafish. (A) Chromatograms of wild-type (WT) zebrafish *pink1* sequence (upper panel) and homozygous Y431* *pink1* sequence (lower panel), with T>G change at position 1,405 in NM_001008628, highlighted in purple. (B) Comparison of the human PINK1 (top, MTS = mitochondrial target sequence) and WT zebrafish (middle) PINK1 protein structure as well as the truncated PINK1^{Y431*} protein (bottom). (C) TcPINK1 Y419X mutation (equivalent to zebrafish Y431X) leads to loss of kinase activity against parkin ubiquitinlike (Ubl) domain. Y419X TcPINK1 (TcY419X) was assayed in parallel with WT TcPINK1 (TcWT) and kinase-inactive TcPINK1 (TcKI). (D) Quantitative polymerase chain reaction of *pink1* transcript levels in *wt* and *pink1*$^{-/-}$ embryos; *wt* levels were normalized to 100%, whereas those from *pink1*$^{-/-}$ embryos were expressed as a percentage of this. In *pink1*$^{-/-}$ embryos, the *pink1* transcript was reduced by approximately 65% (±5%, ****$p < 0.0001$) compared to *wt*. This suggests that the Y431* mutation causes nonsense-mediated decay of *pink1* mRNA, thus further confirming that the Y431* mutation results in loss of function of PINK1.

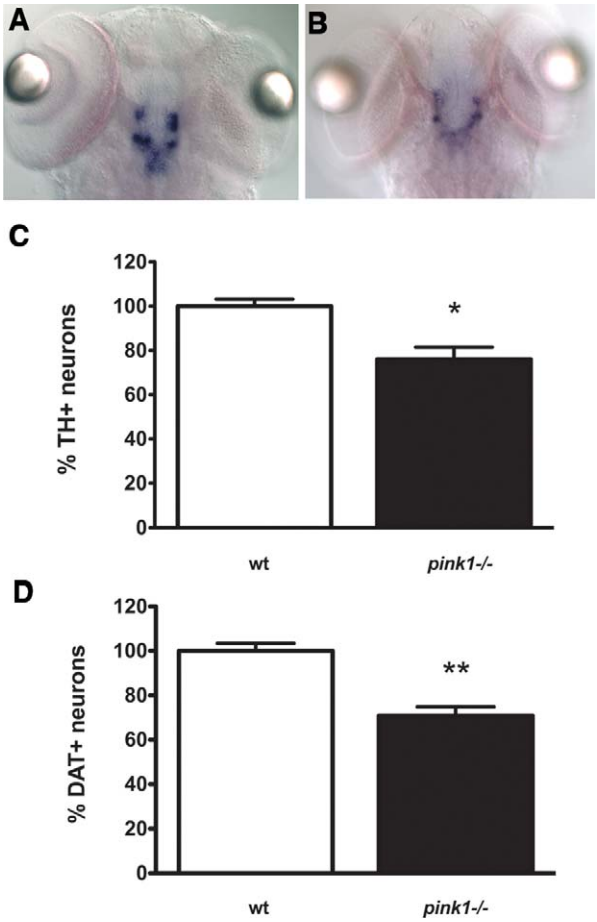

FIGURE 2: Loss of dopaminergic neurons in *pink1*$^{-/-}$ larvae. Representative examples of *wt* (A) and *pink1*$^{-/-}$ larvae (B) after in situ hybridization with a tyrosine hydroxylase (TH) probe at 5 days postfertilization. Purple coloration indicates TH^{+} cells in the brain. *Pink1*$^{-/-}$ larvae had a lower number of dopaminergic neurons in Rink–Wullimann groups 1,2, 4, and 5 (C; *$p < 0.05$, 2-tailed, unpaired *t* test using Welch's correction). The loss of dopaminergic neurons was confirmed using a dopamine transport protein (DAT) probe as a further in situ marker for dopaminergic neurons (D; **$p < 0.01$).

decline in the number of ascending dopaminergic neurons from ~25% reduction at 5 dpf to ~50% in 18-month-old adults could indicate a progressive loss of these ascending dopaminergic neurons in *pink1* mutants from early development to adulthood, but additional experiments determining the number of dopaminergic neurons at multiple time points throughout development and adulthood are necessary to confirm or refute a progressive nature of the observed neuronal cell loss.

The Effect of PINK1 Deficiency Is Highly Specific

Anichtchik et al previously reported that morpholino antisense mediate knockdown of *pink1* in zebrafish embryos resulted in a "severe developmental phenotype" with major generalized neurodevelopmental abnormalities.[10] In contrast, our *pink1*$^{-/-}$ embryos did not display any overt morphological abnormalities. To investigate further the effect of PINK1 deficiency on crucial neurodevelopmental pathways, detailed in situ expression analysis was performed, using a panel of neurodevelopmental markers that included *Emx1* (expression predominantly in ventricular zone and mantle of telencephalon), *shh* (ventral diencephalon, hypothalamus, basal plate, and floor plate), *Pax2.1* (midbrain–hindbrain boundary), *Krox20* (rhombomeres 3 and 5), and *Otpa-Otpb* (dopaminergic neurons in the diencephalon).[23–28] Both the spatiotemporal expression patterns and the intensities were identical for all neurodevelopmental markers in *pink*$^{-/-}$ and *wt* embryos (Supplementary Fig 5). These data imply that the loss of PINK1 activity caused by mutational inactivation of the endogenous gene product does not cause widespread and nonspecific early neurodevelopmental abnormalities. Additional Islet-1 staining of motor neurons was identical in *wt* and *pink*$^{-/-}$ embryos, further supporting our assumption that PINK1 deficiency predominantly exerts its effect on dopaminergic neurons (Supplementary Fig 6).

Pink1$^{-/-}$ *Mutants Have Reduced Mitochondrial Complex I and III Activity*

Because mitochondrial dysfunction is a key factor in the pathogenesis of human *PINK1*-linked PD, we assayed mitochondrial activity in *pink1*$^{-/-}$ larvae. Complex I

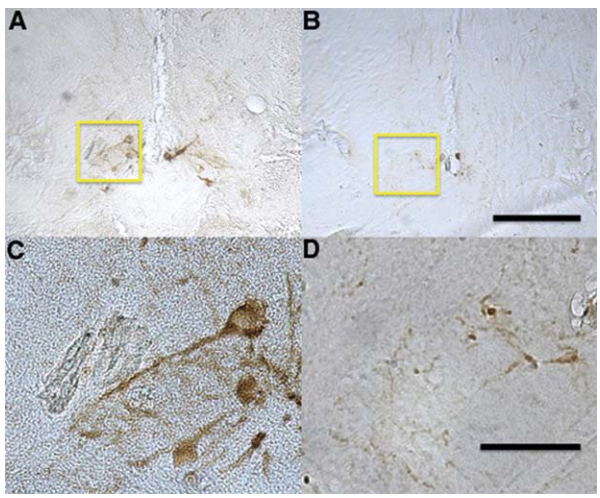

FIGURE 3: Marked loss of dopaminergic neurons in *pink1*$^{-/-}$ adult brain. Representative axial sections of the DC4 cluster in *wt* (A) and *pink1*$^{-/-}$ (B) adult brains are shown stained with anti–tyrosine hydroxylase antibody. (C, D) Enlarged images of A and B (area within *yellow box*), respectively. There is marked reduction in the number of dopaminergic neurons in the DC4 cluster of *pink1*$^{-/-}$ brains ($p < 0.01$, 2-way analysis of variance). Scale bars = 200μm (A, B) and 50μm (C, D).

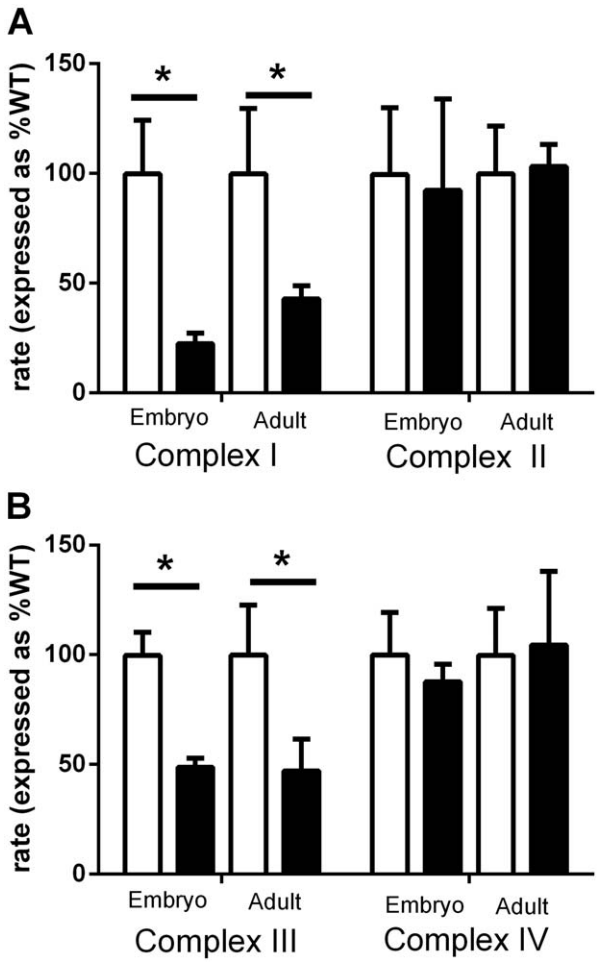

FIGURE 4: *Pink1*$^{-/-}$ zebrafish have similar complex I and III deficiency in early development and adult tissue. Activity of individual mitochondrial complexes measured relative to the mitochondrial marker enzyme citrate synthase and expressed as percentage wild type (%WT), in *wt (white bars)* and *pink1*$^{-/-}$ *(black bars)* embryos at 5 days postfertilization as well as *wt* and *pink1*$^{-/-}$ adult muscle tissue. Complex I and complex III activity in *pink1*$^{-/-}$ embryos is significantly lowered (*$p < 0.05$); this defect is still present in adult *pink1*$^{-/-}$ muscle (*$p < 0.05$). However, the magnitude of the defect does not change when comparison is made between *pink1*$^{-/-}$ embryos and *pink1*$^{-/-}$ adult zebrafish (complex I, $p = 0.09$; complex III, $p = 0.7$). Complex II and IV activity remain unchanged in both *pink1*$^{-/-}$ embryos and *pink1*$^{-/-}$ mutant adults.

activity was reduced by 78% in *pink1*$^{-/-}$ larvae compared to *wt* siblings ($p < 0.05$; mean ± standard deviation: *wt* 2.17 ± 0.5, *pink1*$^{-/-}$ 0.49 ± 0.1). Complex III activity was also reduced by 50% ($p < 0.05$; *wt* 695.2 ± 125, *pink1*$^{-/-}$ 342.4 ± 51.2). In contrast, complex II activity (*wt* 0.55 ± 0.12, *pink1*$^{-/-}$ 0.51 ± 0.13, $p > 0.05$) and complex IV activity (*wt* 537.1 ± 81.9, *pink1*$^{-/-}$ 471.1 ± 74.6, $p > 0.05$) were similar in *wt* and *pink1*$^{-/-}$ larvae (Fig 4).

We next investigated whether mitochondrial dysfunction might increase with ageing by assessing mitochondrial respiratory chain activity in muscle tissue of 2-year-old *pink*$^{-/-}$ zebrafish. Neither complex I nor complex III activity showed a further decrease (complex I: *wt* 3.44 ± 0.75, *pink1*$^{-/-}$ 1.47 ± 0.5; complex III: *wt* 296.74 ± 67.1, *pink1*$^{-/-}$ 140.5 ± 43.3, $p < 0.05$ when compared to adult *wt*, $p > 0.05$ when compared to *pink*$^{-/-}$ larvae; see Fig 4). Similarly, complex II and complex IV activity remained at comparable levels in *pink*$^{-/-}$ and *wt* adults (complex II: *wt* 2.5 ± 0.7, *pink1*$^{-/-}$ 2.6 ± 0.6; complex IV: *wt* 247.3 ± 53.2, *pink1*$^{-/-}$ 258.6 ± 82.9).

Mitochondrial Morphology

At 5 dpf, the density or number of mitochondria per area did not differ significantly between *pink1*$^{-/-}$ and *wt* (ratio 0.52 ± 0.13 for mitochondrial area/total area in *pink1*$^{-/-}$ vs 0.58 ± 0.09 for *wt*). However, individual mitochondria were on average 40% larger compared to *wt* (*pink1*$^{-/-}$ 0.69μm^2, n = 175, per mitochondrial section vs *wt* 0.49μm^2, n = 174, $p < 0.05$; Fig 5A, B). We also observed an increase (~47%) in the average mitochondrial area per section in *pink1*$^{-/-}$ mutant adults (*pink1*$^{-/-}$ 1.37μm^2 per mitochondrial section [n = 228] vs *wt* 0.93μm^2 [n = 231], $p < 0.05$; see Fig 5C, D). Taking these data together, we conclude that PINK1 deficiency results in moderate yet significant alterations in mitochondrial ultrastructure. Similar to the changes in mitochondrial function, the increase in mitochondrial size is already present during early development and is not further exacerbated through adulthood.

TigarB Upregulation in Pink1$^{-/-}$ *Larvae*

We next hypothesized that the observed mitochondrial dysfunction and loss of dopaminergic neurons in *pink1*$^{-/-}$ larvae might be influenced by changes in gene expression. Using an unbiased, array-based, genome-wide gene expression analysis approach, we identified 274 probes with >2-fold change and $p < 0.01$ (when corrected for multiple comparisons). One hundred sixteen probes/108 genes were upregulated (higher in *pink1*$^{-/-}$ than *wt*), and 158 probes/146 genes were downregulated (lower in *pink1*$^{-/-}$ than in *wt*; Supplementary Table).

TigarB (ENSDARG00000045858), an orthologue of *TIGAR* (ENST00000179259), shares 40% protein homology and 62% transcript homology to the human gene and was upregulated more than 12-fold in *pink1*$^{-/-}$ embryos in the initial gene array experiments. *TigarB* mRNA levels were also increased in *pink1*$^{-/-}$ embryos in the confirmatory qPCR experiments when compared to *wt* after normalization to the housekeeping gene *EF1alpha* (2.5-fold upregulation, $p = 0.0003$). Whole mount in situ hybridization analysis revealed a

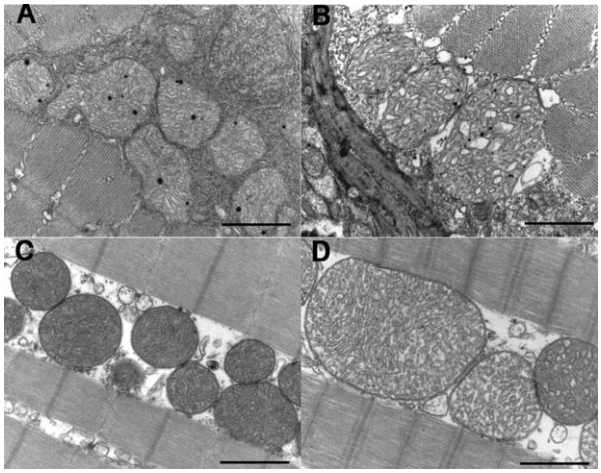

FIGURE 5: Mitochondria are enlarged in both larval (B) and adult (D) *pink1*$^{-/-}$ tissue compared to larval (A) or adult (C) *wt* control tissue. Electron microscopy sections of muscle tissue in 5-day-old zebrafish larvae and 2-year-old adult zebrafish are shown. The average size of the mitochondria was larger in both *pink1*$^{-/-}$ larvae and adult tissue ($p < 0.01$; 2-sided Student *t* test). In adult *pink1*$^{-/-}$ tissue, some mitochondria had considerably higher electron density than others (D).

marked upregulation of TigarB in *pink1*$^{-/-}$ brains as early as 24 hpf (Fig 6). Zebrafish possess an additional *TIGAR* orthologue, *TigarA* (ENSDARG00000051749), which shares 40% protein homology with the human TIGAR gene, but this transcript did not show a change in the microarray experiments (data not shown).

To investigate the functional significance of *TigarB* upregulation, an MO (TBMO2) designed to disrupt *TigarB* splicing was injected into single cell stage *pink1*$^{-/-}$ embryos and *wt* controls (see Supplementary Fig 1). This MO-mediated inactivation of TigarB resulted in complete rescue of dopaminergic neurons in *pink1*$^{-/-}$ larvae at 3 dpf (Fig 7, top). To further validate the rescue effect of *TigarB* knockdown in PINK1 deficiency, confirmatory double-knockdown experiments were undertaken in *wt* zebrafish embryos. Coinjections were undertaken with PINK5, an MO directed against the exon–intron boundary of exon 5, and the TigarB MO TBMO2. PINK5 MO-mediated *pink1* knockdown led to a reduction of the dopaminergic neurons by approximately 20% at 3 dpf ($p = 0.01$), similar to the observed reduction of dopaminergic neurons in the stable *pink1* mutant line. Coinjection of the MOs PINK5 and TBMO2 again completely rescued the dopaminergic neurons (see Fig 7, bottom).

We hypothesized that this rescue may be due to normalization of mitochondrial function after *TigarB* inactivation and therefore assessed the activity of the individual complexes of the mitochondrial respiratory chain in *pink1*$^{-/-}$ larvae. As predicted, both complex I activity and complex III activity were normalized in *pink1*$^{-/-}$ larvae after *TigarB* inactivation (Fig 8).

Microglial Activation

Abnormal expression of innate immunity genes precedes dopaminergic deficits in PINK1-deficient mice.[29] Moderate microgliosis was reported in the only postmortem report on a brain of a PD patient with 2 *PINK1* mutations.[30] Of note, several of the markedly upregulated genes in our gene expression analysis (see see Supplementary Table), such as complement factor H and calpain, are involved in immune mechanisms and activation of microglial cells.[31] Using an ApoE in situ probe as a microglial marker, we compared the number of microglial cells in *wt* and *pink1*$^{-/-}$ zebrafish larvae.[17] There was a marked increase in microglial activation in the *pink1*$^{-/-}$ embryos at 3 dpf (*pink1*$^{-/-}$ 32.3 $\pm$ 4.7 microglial cells per embryo, *wt* 20.0 $\pm$ 0.82, $p < 0.05$; Fig 9). Microglial development can be completely abolished in zebrafish embryos using an MO targeting the transcription factor *pu.1* (Supplementary Fig 7).[32] We postulated that inactivation of microglia resulting from MO-mediated *pu.1* knockdown might have a protective effect on the dopaminergic neurons in the *pink1*$^{-/-}$ embryos. However, there was no difference in the number of dopaminergic neurons between uninjected and *pu.1* MO-injected *pink1*$^{-/-}$ larvae (number of dopaminergic neurons in *pu.1* MO-injected *pink1*$^{-/-}$ embryos: 26.5 $\pm$ 1.36; number of dopaminergic neurons in uninjected *pink1*$^{-/-}$ embryos: 25.0 $\pm$ 1.55, $p > 0.05$). This suggests that the observed microglial activation may be a downstream mechanism involved in clearing already damaged or dead dopaminergic neurons, rather than a crucial upstream mechanism leading to the loss of dopaminergic neurons in PINK1 deficiency.

Discussion

Genetic research has provided crucial new insight into the pathogenesis of PD, but the precise mechanisms leading

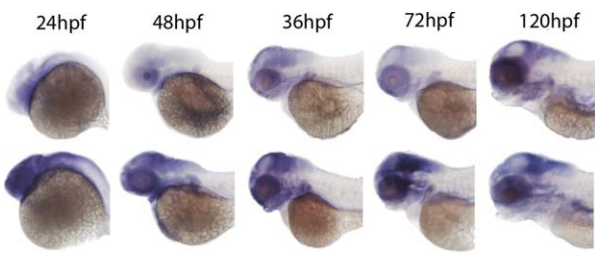

FIGURE 6: *TigarB* is expressed in brain tissue and upregulated in *pink1*$^{-/-}$. Whole mount in situ hybridization was performed using a riboprobe specific for *TigarB* expression. *TigarB* expression was largely limited to the brain. *Pink1*$^{-/-}$ embryos show a marked increase in *TigarB* expression (bottom panels) compared to *wt* (top panels) throughout development. hpf = hours postfertilization.

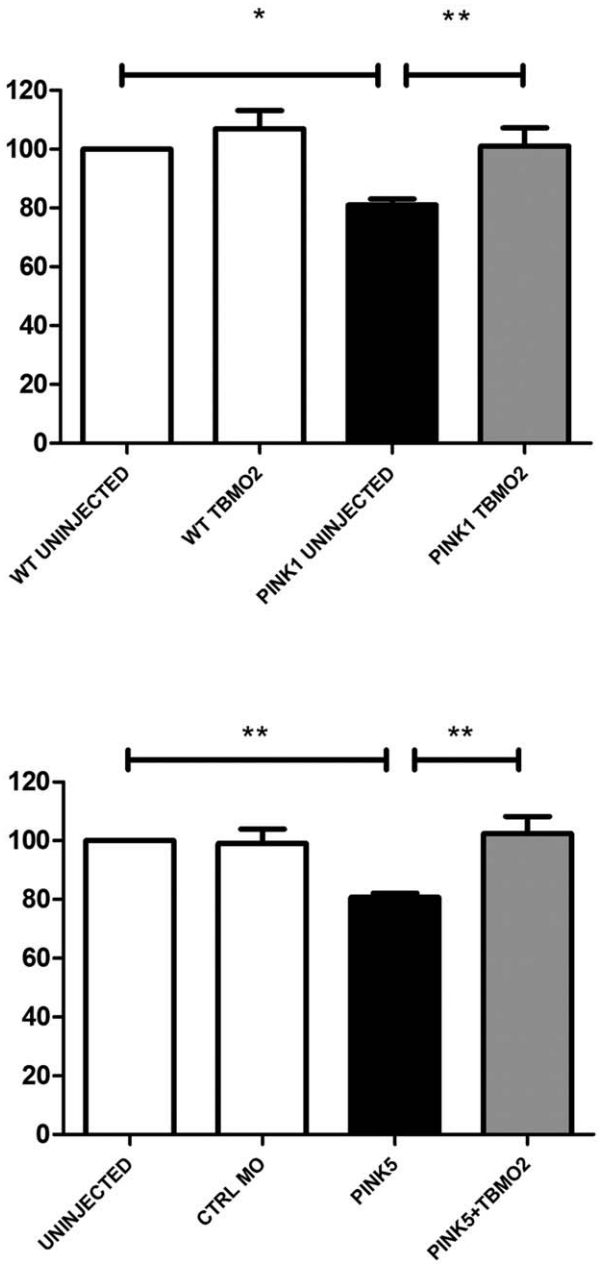

FIGURE 7: Morpholino antisense oligonucleotide (MO)-mediated knockdown of *TigarB* results in rescue of dopaminergic neurons. Tyrosine hydroxylase neurons were counted at 3 days postfertilization (dpf) and expressed as a percentage of *wt* uninjected mean. *TigarB* knockdown in *wt* embryos (30 ± 2.92, WT TBMO2) resulted in a small increase of 5% compared to *wt* uninjected (28 ± 1.21, WT), but this did not reach statistical significance ($p > 0.05$). The *pink1*$^{-/-}$ uninjected embryos displayed a similar decrease in the number of dopaminergic neurons (22.8 ± 1.3, PINK1$^{-/-}$) as observed at 5 dpf (see Fig 2) of approximately 20% (*$p = 0.04$, PINK1$^{-/-}$), but MO knockdown of *TigarB* in *pink1*$^{-/-}$ embryos completely rescued the dopaminergic neurons (29.2 ± 2.6, **$p = 0.01$, PINK1 TBMO2, top panel). In confirmatory experiments, coinjections of an MO directed against *pink1* (PINK5) and Tigar (TBMO2) again completely rescued the dopaminergic neurons in pink1-deficient zebrafish embryos (bottom, **$p < 0.01$).

to neuronal cell death remain to be elucidated.[33] Recessive loss of function mutations in autosomal genes such as parkin, *PINK1,* or *DJ-1* are associated with inherited forms of EOPD. Conditional knockout of parkin in adult rodents leads to progressive loss of dopaminergic neurons, but classical parkin, *Pink1,* or *DJ-1* knockout mice do not develop loss of dopaminergic neurons, hampering investigation of their pathogenic effects especially in early stages of brain development.[6,34] By contrast, our *pink*$^{-/-}$ zebrafish display loss of dopaminergic neurons as well as other key features of the disease, such as impaired mitochondrial function and morphology as early as 5 dpf, thus providing a tractable vertebrate genetic model for EOPD. The

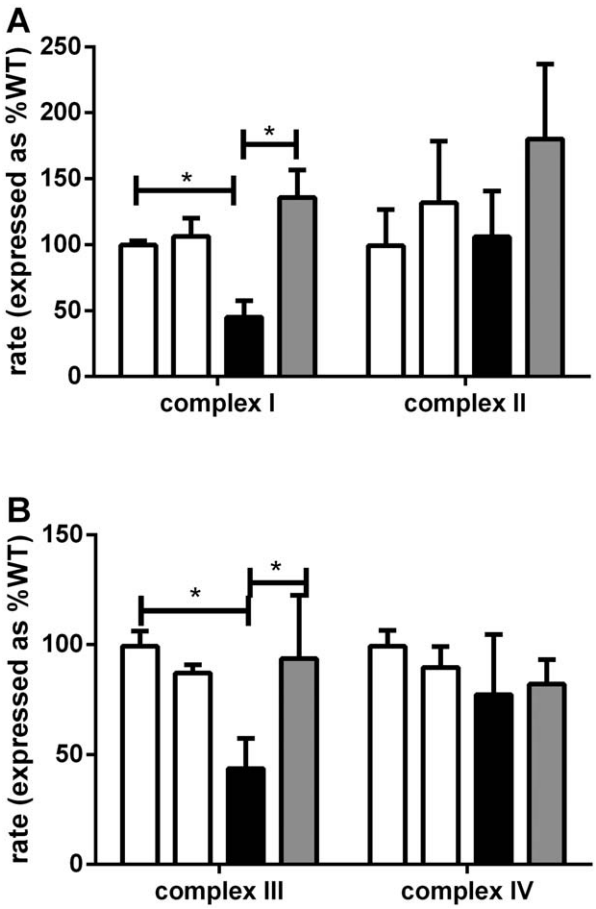

FIGURE 8: Spectrophotometric measurement of complex I activity was lower by 55% in *pink1*$^{-/-}$ zebrafish *(black bars)* compared to *wt* sibling embryos *(white bars)* at 3 days postfertilization, and recovered to normal levels in *pink1*$^{-/-}$ zebrafish with *TigarB* knockdown (*gray bars; wt* 8.07 ± 0.25, *wt* with *TigarB* knockdown *[second white bar]* 8.618 ± 1.11, *pink1*$^{-/-}$ 3.67 ± 0.99, *pink1*$^{-/-}$ *TigarB* morpholino antisense oligonucleotide 10.98 ± 1.67, *$p < 0.05$). Complex III activity was similarly reduced by 55% in *pink1*$^{-/-}$ zebrafish compared to *wt* sibling embryos, and recovered to normal levels in *pink1*$^{-/-}$ zebrafish with *TigarB* knockdown (*wt* 796 ± 52, *wt* with *TigarB* knockdown 695 ± 29, *pink1*$^{-/-}$ 351 ± 106, *pink1*$^{-/-}$ with *TigarB* knockdown 749 ± 228, *$p < 0.05$).

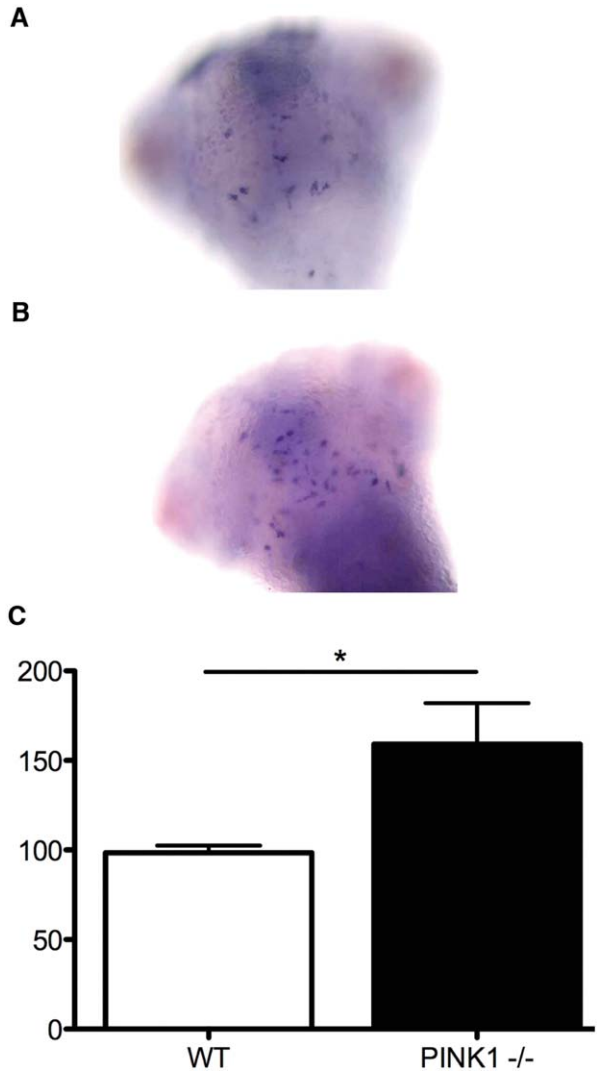

FIGURE 9: Marked microglial activation in *pink1*$^{-/-}$ embryos. Whole mount in situ hybridization using a riboprobe specific for apolipoprotein E revealed marked increase of activated microglia in *pink1*$^{-/-}$ compared to *wt* at 5 days postfertilization (A: *wt*; B: *pink1*$^{-/-}$; C: quantitative analysis, **p* < 0.05, *t* test; please note that A and B were contrast-enhanced for illustrative purposes).

precise projection of the dopaminergic neurons in the posterior tuberculum is still a matter of debate.[20,35,36] However, all studies using zebrafish as an animal model for PD have universally observed a loss of dopaminergic neurons in the posterior tuberculum after PD toxin exposure such as treatment with MPP+ and frequently also after MO-mediated transient PD gene knockdown.[11,37] The functional relevance of the Y431X mutation was confirmed in kinase activity assays but also by studying the effect of this Y431X mutation on *pink1* transcript levels.

Importantly, our data also suggest that both mitochondrial dysfunction and changes in mitochondrial morphology are early, specific consequences of PINK1 deficiency that do not progress further with age.

TIGAR is a bisphosphatase that lowers fructose-2,6-biphosphate (Fru-2,6-P2) levels in cells, resulting in an inhibition of glycolysis and an overall decrease in intracellular reactive oxygen species via increased production of nicotinamide adenine dinucleotide phosphate through the pentose phosphate shunt.[13] Recombinant human and zebrafish TIGAR have similar catalytic activity.[38] Increased substrate provision normalizes impaired mitochondrial respiration in PINK1 deficiency.[39] Further studies are needed to determine whether decreased substrate provision for mitochondrial respiration via TIGAR-mediated inhibition of glycolysis may contribute to this relative substrate deficiency in the absence of PINK function. More recently, TIGAR has also been identified as a negative regulator of mitophagy.[40] TIGAR upregulation results in an increased number of enlarged mitochondria in mice, comparable to the mitochondrial enlargement identified in our *pink1*$^{-/-}$ zebrafish.[40] Impaired mitophagy is currently considered to be a crucial mechanism in the pathogenesis of early onset PD.[41] The observed *TigarB* upregulation in *pink1*$^{-/-}$ zebrafish now suggests that additional mechanisms other than impaired PINK1-mediated recruitment of parkin to damaged mitochondria may contribute to impaired mitophagy in PD.[42] The rescue of dopaminergic neurons in *pink1*$^{-/-}$ zebrafish after TigarB inactivation was confirmed using a complementary, MO-mediated *pink1* knockdown approach.

The complete normalization of mitochondrial function and resulting rescue of ascending dopaminergic neurons after antisense-mediated *TigarB* inactivation suggests that modulation of TIGAR-mediated mechanisms may be a promising strategy for disease-modifying therapy. TIGAR is typically activated by p53. Our data therefore provide a further intriguing link between neurodegeneration and cancer-related mechanisms.[43,44]

Both the extent of microglial activation and the lack of a protective effect of microglia on the loss of the dopaminergic neurons in *pink1*$^{-/-}$ embryos were somewhat surprising. Our data suggest that microglial activation is—at least in this model—more likely to reflect either nonspecific activation or a limited role for microglia in the clearing of cell debris.

Acknowledgment

Financial support from Parkinson's UK (G-0608; G-0901) BBSRC/Lilly (PhD CASE studentship, BB/I532553/1) and Sheffield Hospitals Charitable Trust (7884) for O.B. and from the Medical Research Council (MRC) to P.W.I. is gratefully acknowledged. This work was also supported by the Cluster of Excellence Frankfurt Macromolecular Complexes at the Goethe University

Frankfurt DFG project EXC 115, the DFG grant RE1575-1/1 (A.S.R.), and the Humboldt Association (R.W.K.). M.M.K.M. is funded by a Wellcome Intermediate Clinical Fellowship (083601/Z/07/Z); Parkinson's UK; the Michael J. Fox Foundation for Parkinson's Research; a Wellcome/MRC PD consortium grant to the University College London Institute of Neurology, University of Sheffield, and MRC Protein Phosphorylation and Ubiquitylation Unit of the University of Dundee; and the pharmaceutical companies supporting the Division of Signal Transduction Therapy Unit (AstraZeneca, Boehringer Ingelheim, GlaxoSmithKline, Merck, Janssen Pharmaceutica, and Pfizer).

The sequence analysis that led to the identification of the *pink1*^{Y431*} mutation was undertaken at the Wellcome Sanger Institute, Cambridge by Drs R. Kettleborough and D. Stemple.

We thank Drs W Driever, F Peri, KB Rohr, and G De Rienzo for sharing in situ probes with us; L. Jennen for preparing electron microscopy sections and recordings; the aquarium staff at the MRC Centre for Developmental and Medical Genetics, University of Sheffield; and Dr M. Peggie for generating plasmid cDNA clones for expression of zebrafish and *Tribolium castaneum* PINK1. We would also like to acknowledge technical assistance by Dr Huw Jones.

Authorship

L.J.F. and M.K. contributed equally to this article.

Potential Conflicts of Interest

Nothing to report.

References

1. Valente EM, Abou-Sleiman PM, Caputo V, et al. Hereditary early-onset Parkinson's disease caused by mutations in PINK1. Science 2004;21: 304:1158–1160.
2. Gandhi S, Muqit MM, Stanyer L, et al. PINK1 protein in normal human brain and Parkinson's disease. Brain 2006;129:1720–1731.
3. Hoepken HH, Gispert S, Morales B, et al. Mitochondrial dysfunction, peroxidation damage and changes in glutathione metabolism in PARK6. Neurobiol Dis 2007;25:401–411.
4. Morais VA, Verstreken P, Roethig A, et al. Parkinson's disease mutations in PINK1 result in decreased Complex I activity and deficient synaptic function. EMBO Mol Med 2009;1:99–111.
5. Gautier CA, Kitada T, Shen J. Loss of PINK1 causes mitochondrial functional defects and increased sensitivity to oxidative stress. Proc Natl Acad Sci U S A 2008;105:11364–11369.
6. Dawson TM, Ko HS, Dawson VL. Genetic animal models of Parkinson's disease. Neuron 2010;66:646–661.
7. Bandmann O, Burton EA. Genetic zebrafish models of neurodegenerative diseases. Neurobiol Dis 2010;40:58–65.
8. Panula P, Chen YC, Priyadarshini M, et al. The comparative neuroanatomy and neurochemistry of zebrafish CNS systems of relevance to human neuropsychiatric diseases. Neurobiol Dis 2010;40: 46–57.
9. Bill BR, Petzold AM, Clark KJ, et al. A primer for morpholino use in zebrafish. Zebrafish 2009;6:69–77.
10. Anichtchik O, Diekmann H, Fleming A, et al. Loss of PINK1 function affects development and results in neurodegeneration in zebrafish. J Neurosci 2008;28:8199–8207.
11. Sallinen V, Kolehmainen J, Priyadarshini M, et al. Dopaminergic cell damage and vulnerability to MPTP in Pink1 knockdown zebrafish. Neurobiol Dis 2010;40:93–101.
12. Xi Y, Ryan J, Noble S, et al. Impaired dopaminergic neuron development and locomotor function in zebrafish with loss of pink1 function. Eur J Neurosci 2010;31:623–633.
13. Bensaad K, Tsuruta A, Selak MA, et al. TIGAR, a p53-inducible regulator of glycolysis and apoptosis. Cell 2006;126:107–120.
14. Woodroof HI, Pogson JH, Begley M, et al. Discovery of catalytically active orthologues of the Parkinson's disease kinase PINK1: analysis of substrate specificity and impact of mutations. Open Biol 2011;1:110012.
15. Thisse C, Thisse B. High-resolution in situ hybridization to whole-mount zebrafish embryos. Nat Protoc 2008;3:59–69.
16. Flinn L, Mortiboys H, Volkmann K, et al. Complex I deficiency and dopaminergic neuronal cell loss in parkin-deficient zebrafish (Danio rerio). Brain 2009;132:1613–1623.
17. Peri F, Nusslein-Volhard C. Live imaging of neuronal degradation by microglia reveals a role for v0-ATPase a1 in phagosomal fusion in vivo. Cell 2008;133:916–927.
18. Su F, Juarez MA, Cooke CL, et al. Differential regulation of primitive myelopoiesis in the zebrafish by Spi-1/Pu.1 and C/ebp1. Zebrafish 2007;4:187–199.
19. Kondapalli C, Kazlauskaite A, Zhang N, et al. PINK1 is activated by mitochondrial membrane potential depolarization and stimulates Parkin E3 ligase activity by phosphorylating Serine 65. Open Biol 2012;2:120080.
20. Rink E, Wullimann MF. The teleostean (zebrafish) dopaminergic system ascending to the subpallium (striatum) is located in the basal diencephalon (posterior tuberculum). Brain Res 2001;889:316–330.
21. Rink E, Wullimann MF. Connections of the ventral telencephalon and tyrosine hydroxylase distribution in the zebrafish brain (Danio rerio) lead to identification of an ascending dopaminergic system in a teleost. Brain Res Bull 2002;57:385–387.
22. Schweitzer J, Lohr H, Filippi A, Driever W. Dopaminergic and noradrenergic circuit development in zebrafish. Dev Neurobiol 2012; 72:256–268.
23. Del Giacco L, Sordino P, Pistocchi A, et al. Differential regulation of the zebrafish orthopedia 1 gene during fate determination of diencephalic neurons. BMC Dev Biol 2006;6:50.
24. Pfeffer PL, Gerster T, Lun K, et al. Characterization of three novel members of the zebrafish Pax2/5/8 family: dependency of Pax5 and Pax8 expression on the Pax2.1 (noi) function. Development 1998;125:3063–3074.
25. Ryu S, Mahler J, Acampora D, et al. Orthopedia homeodomain protein is essential for diencephalic dopaminergic neuron development. Curr Biol 2007;17:873–880.
26. Scholpp S, Wolf O, Brand M, Lumsden A. Hedgehog signalling from the zona limitans intrathalamica orchestrates patterning of the zebrafish diencephalon. Development 2006;133:855–864.
27. Viktorin G, Chiuchitu C, Rissler M, et al. Emx3 is required for the differentiation of dorsal telencephalic neurons. Dev Dyn 2009;238: 1984–1998.

28. Voiculescu O, Taillebourg E, Pujades C, et al. Hindbrain patterning: Krox20 couples segmentation and specification of regional identity. Development 2001;128:4967–4978.

29. Akundi RS, Huang Z, Eason J, et al. Increased mitochondrial calcium sensitivity and abnormal expression of innate immunity genes precede dopaminergic defects in Pink1-deficient mice. PLoS One 2011;6:e16038.

30. Samaranch L, Lorenzo-Betancor O, Arbelo JM, et al. PINK1-linked parkinsonism is associated with Lewy body pathology. Brain 2010; 133(pt 4):1128–1142.

31. Levesque S, Wilson B, Gregoria V, et al. Reactive microgliosis: extracellular micro-calpain and microglia-mediated dopaminergic neurotoxicity. Brain 2010;133(pt 3):808–821.

32. Rhodes J, Hagen A, Hsu K, et al. Interplay of pu.1 and gata1 determines myelo-erythroid progenitor cell fate in zebrafish. Dev Cell 2005;8:97–108.

33. Hardy J. Genetic analysis of pathways to Parkinson disease. Neuron 2010;68:201–206.

34. Shin JH, Ko HS, Kang H, et al. PARIS (ZNF746) repression of PGC-1alpha contributes to neurodegeneration in Parkinson's disease. Cell 2011;144:689–702.

35. Rink E, Wullimann MF. Development of the catecholaminergic system in the early zebrafish brain: an immunohistochemical study. Brain Res Dev Brain Res 2002;137:89–100.

36. Tay TL, Ronneberger O, Ryu S, et al. Comprehensive catecholaminergic projectome analysis reveals single-neuron integration of zebrafish ascending and descending dopaminergic systems. Nat Commun 2011;25: 2:171.

37. Bretaud S, Lee S, Guo S. Sensitivity of zebrafish to environmental toxins implicated in Parkinson's disease. Neurotoxicol Teratol 2004;26:857–864.

38. Li H, Jogl G. Structural and biochemical studies of TIGAR (TP53-induced glycolysis and apoptosis regulator). J Biol Chem 2009; 284:1748–1754.

39. Gandhi S, Wood-Kaczmar A, Yao Z, et al. PINK1-associated Parkinson's disease is caused by neuronal vulnerability to calcium-induced cell death. Mol Cell 2009;33:627–638.

40. Hoshino A, Matoba S, Iwai-Kanai E, et al. p53-TIGAR axis attenuates mitophagy to exacerbate cardiac damage after ischemia. J Mol Cell Cardiol 2012;52:175–184.

41. Vives-Bauza C, Przedborski S. Mitophagy: the latest problem for Parkinson's disease. Trends Mol Med 2011;17:158–165.

42. Narendra DP, Jin SM, Tanaka A, et al. PINK1 is selectively stabilized on impaired mitochondria to activate Parkin. PLoS Biol 2010; 8:e1000298.

43. Green DR, Chipuk JE. p53 and metabolism: inside the TIGAR. Cell 2006;126:30–32.

44. Plun-Favreau H, Lewis PA, Hardy J, et al. Cancer and neurodegeneration: between the devil and the deep blue sea. PLoS Genet 2010;6:e1001257.